An Electron Microscopy Study of Modes of Intermetallic Precipitation in Ti-Cu Alloys

J. C. WILLIAMS, R. TAGGART, AND D. H. POLONIS

The precipitation processes that accompany the aging of supersaturated α-titanium solid solutions containing up to 6 wt pct Cu have been studied by thin foil electron microscopy and X-ray diffraction techniques. Two mechanisms of decomposition have been identified: i) the heterogeneous nucleation and growth of Ti_2Cu at interfaces and internal substructure such as dislocations, and ii) the uniform nucleation of thin, coherent, disk-shaped precipitates which lie on $\{10\bar{1}1\}$. The coherent precipitates can form with densities up to 10^{17} per cu cm; this and many morphological features of the precipitation process in Ti-Cu are analogous to the well-known behavior of Al-Cu alloys. The coherent precipitates first lose coherency along the edge of the disk and then along the flat faces. The mechanisms by which these two processes occur are considered in detail.

THE precipitation of intermetallic compounds from supersaturated solid solutions of the hexagonal α-phase in titanium alloys has considerable potential for developing materials with high yield strengths. The available literature indicates that such precipitation reactions have not been studied in detail.

The strengthening of Ti-Cu alloys by intermetallic compound precipitation has been examined by D. N. Williams, *et al.*[1] These workers showed that annealing at 760°C resulted in some strengthening but the strength levels attained were not high enough to be commercially promising. More recently Gallaugher, Taggart, and Polonis[2] have reported significant increases in microhardness during aging at temperatures up to 550°C and that rapid overaging occurs even at 550°C. A comparison of these results with the earlier results of Williams, *et al.* shows that strengths reported for samples aged at 760°C represent gross overaged properties.

The present work is concerned with intermetallic compound precipitation in α-phase titanium alloys that are supersaturated with respect to copper. These supersaturations have been obtained by quenching from solution temperatures at which the copper content of an alloy is dissolved in the α-phase or by quenching from the β-phase field to produce the hexagonal α' titanium martensite which is supersaturated in copper. During the subsequent aging of these quenched alloys, precipitation reactions occur which lead to the formation of the equilibrium Ti_2Cu intermetallic compound. The details of this precipitation reaction have been investigated by employing transmission electron microscopy, selected area electron diffraction and X-ray diffraction techniques.

EXPERIMENTAL METHODS

The alloys were prepared using conventional nonconsumable electrode arc melting techniques. Each button was melted on alternate sides a total of twelve times; the buttons were wrapped in tantalum foil then sealed in evacuated silica capsules, homogenized at 1000°C for one week and cold rolled into 0.020 in. thick strips. Vacuum or argon atmosphere furnaces were used for the solution heat treatments and neutral salt baths were used for the aging treatments.

The chemical analyses of the alloys used in this investigation are shown in Table I. Thin foils were prepared by a technique which has been described in detail elsewhere.[3] All dark field images were obtained using high resolution technique.

EXPERIMENTAL RESULTS

: The decomposition of the supersaturated α-phase during aging at temperatures ranging from 400° to 500°C has been observed to occur by two distinct processes:

a) The heterogeneous nucleation and growth of precipitates, identified as Ti_2Cu, that form at dislocations and other types of martensitic substructures

b) The uniform nucleation of thin, coherent plates of a transition precipitate, the nature of which changes during aging to form incoherent Ti_2Cu after long aging times.

These processes apply to supersaturated solid solutions obtained by quenching from within the α-phase field or by quenching from the β-phase field to produce martensitic α. The maximum solute concentration which can be retained in α-quenched samples is ~1.8 wt pct Cu, whereas solid solutions of up to 8 wt pct Cu are produced by the martensitic transformation of β-

Table I. Alloy Compositions After Melting, Rolling and Solution Heat Treatment

Nominal Copper Content, wt pct*	Oxygen†	Hydrogen†	Nitrogen†
2	320	45	<200
4	290	40	<200
6	280	40	<200
1.8‡	180	10	<100

*Analyses show that all copper contents are within ±0.5 wt pct of nominal.
†Ppm by weight.
‡Levitation melted.

J. C. WILLIAMS, formerly Predoctoral Research Associate, University of Washington, Seattle, Wash., is now Group Leader Physical Metallurgy, Science Center, North American Rockwell Corp., Thousand Oaks, Calif. R. TAGGART and D. H. POLONIS are Professors of Mechanical Engineering and Metallurgical Engineering, respectively, University of Washington.

Manuscript submitted July 2, 1970.

(a)

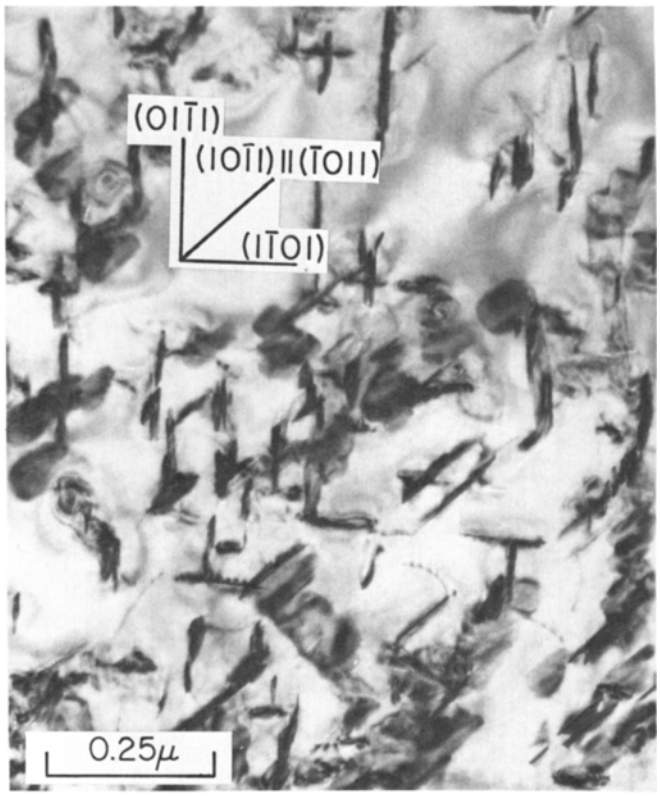

(b)

Fig. 1—(a) Single variant of heterogeneously nucleated Ti_2Cu precipitates at martensite plate boundaries. Ti-2 pct Cu β-quenched and aged at 500°C for 1 hr. (b) Heterogeneously nucleated Ti_2Cu at a type dislocations. Note that in all cases two variants of precipitate form at each dislocation. Ti-4 pct Cu β-quenched and aged 2 hr at 500°C.

quenched samples. The following discussion of the decomposition processes applies equally well to either type of starting material. In general, however, the martensitic α' has a higher density of substructure, the detailed nature of which has been described previously.[4] Thus, the heterogeneous nucleation of precipitates is expected to be more important in samples quenched from the β-phase field. This paper is concerned only with the mechanisms of precipitation; accordingly, the relative importance of the concurrent competing processes is not considered.

A) Heterogeneously Nucleated Precipitates

The heterogenously nucleated precipitates are always observed before the uniformly nucleated, coherent precipitate is detected. The first heterogeneously nucleated precipitates to form are those in the low angle martensite plate boundaries, as shown in Fig. 1(*a*). These precipitates form during quenching and subsequently grow during aging. After short aging times, precipitates are also nucleated at dislocations within the matrix, an example of which is shown in Fig. 1(*b*). Both the precipitates in the boundaries and those at individual dislocations form initially as thin semicoherent disks on $\{10\bar{1}1\}$, the detailed nature of which will be described more completely below. Although the identification of these precipitates by selected area diffraction is difficult because of their small size and low volume fraction, sufficient diffraction evidence has been obtained to indicate that the precipitates are Ti_2Cu.

B) Uniformly Nucleated Precipitates

As the aging process continues, thin, coherent, plate-shaped precipitates are nucleated at sites remote from the dislocations or other structural perturbations such as twin interfaces within the martensite plates, as shown in Fig. 2. This precipitation process has been studied in detail in order to provide information about the structural mechanisms of the process and the over-aging characteristics of the precipitate; the information relevant to each separate feature is listed below.

1) HABIT PLANE

The habit plane of the coherent precipitate has been established at $\{10\bar{1}1\}$ by trace analysis, as shown in Fig. 3, and by the analysis of the streaking that occurs in the selected area diffraction patterns, as shown in Figs. 4(*a*) and (*b*). From these and other patterns it can be seen that the streaks always lie parallel to $\{10\bar{1}1\}$ diffraction vectors, which verified the $\{10\bar{1}1\}$ habit plane of the precipitate.

2) GROWTH

The coherent precipitates are first detectable as small regions ~30 to 40Å along their maximum dimension. The exact morphology at this stage is not clear since a portion of the image may be due to coherency strain contrast in the matrix. After slightly longer aging times the precipitates assume a characteristic disk shape, as shown in Fig. 5. The disk-shaped precipitates are 15 ± 5Å thick and grow preferentially in the radial direction with no detectable thickening. The

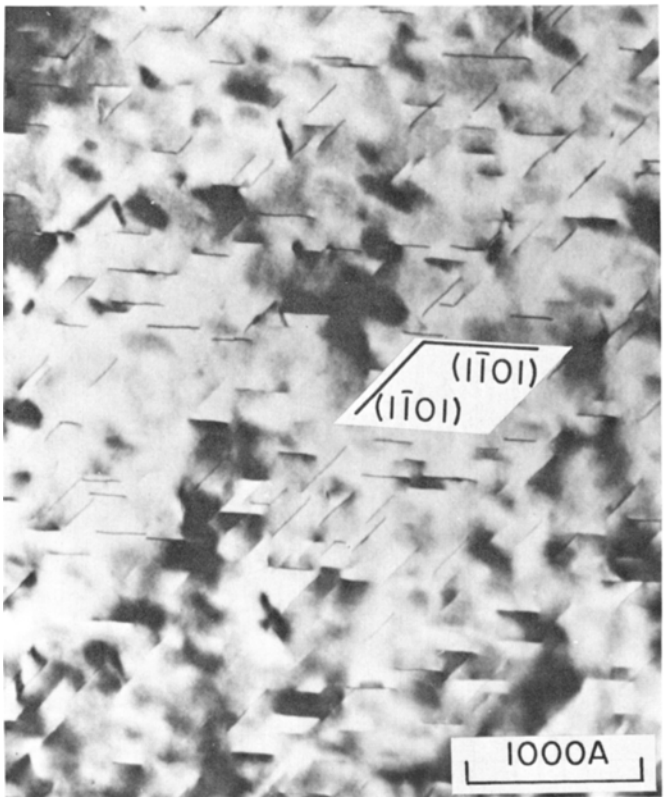

Fig. 2—Thin, coherent, disk-shaped precipitates in a Ti-4 pct Cu alloy β-quenched and aged 72 hr at 450°C.

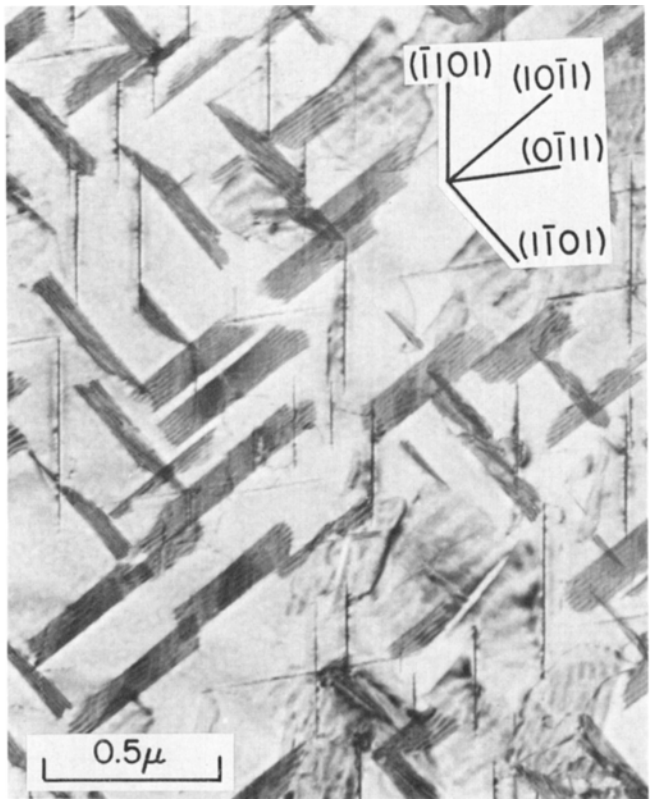

Fig. 3—Larger disk-shaped precipitates showing five distinct variants of the $\{10\bar{1}1\}$ habit plane. The sixth variant is symmetric with the $\{\bar{1}011\}$ trace and is thus indistinguishable. Ti-2 pct Cu α-quenched and aged 48 hr at 500°C.

number of precipitates per unit volume decreases with increased aging temperature in the range 400° to 500°C and with decreased alloy content. At large interparticle spacings the precipitates can grow to diameters in excess of 3500Å, as shown in Fig. 6, while maintaining a constant 15 ± 5Å thickness.

3) CRYSTAL STRUCTURE

No reflections, other than those identified with the alpha phase, are observed in the selected area diffraction patterns shown in Figs. 4(*a*) and (*b*) which were taken from regions containing the fully coherent precipitate. This observation indicates that the precipitate either has the same crystal structure as the matrix, as expected for G. P. zones,[5,6] or that it has a structure which is closely related to the matrix, such as the ω-phase in the β-phase of Ti alloys.[7,8] Additional diffraction patterns that were obtained for the other major hcp zones do not contain extra reflections, thereby excluding the latter possibility. During the later stages of precipitation, when the precipitate is incoherent, selected area diffraction patterns contain numerous extra reflections which can be indexed in terms of the equilibrium bct ($C11_b$ type) Ti_2Cu precipitate, as shown in Fig. 7. From such patterns the orientation relation between α and Ti_2Cu has been established as:

$$(0001)_\alpha \parallel (103)_{Ti_2Cu}$$

$$\langle 11\bar{2}0\rangle_\alpha \parallel \langle 331\rangle_{Ti_2Cu}$$

By comparing Figs. 4(*a*) and 7, it is clear that the coherent precipitates do not have the Ti_2Cu structure since none of the Ti_2Cu reflections shown in Fig. 7 are present in Fig. 4(*a*).

4) MISFIT

The sense of the misfit associated with the coherent precipitates has been evaluated using three types of experimental observations: The displacement of streaks in the selected area diffraction patterns,* Ashby-Brown[9,10] strain contrast from anomalously wide dark field images, and the sense of the misfit vector associated with the displacement fringe contrast observed during the later stages of aging, but while the precipitate is fully coherent. The results of each type of observation are mutually consistent and indicate that the precipitate has a positive misfit (interstitial type). Figs. 8(*a*) and (*b*) show the displacement fringe contrast associated with the precipitates while Fig. 8(*c*) shows in a schematic form the relation between the diffraction vector **g**, the misfit vector **R** and the inclination of the precipitate.

*The relation between the displacement of streaks and the sense of precipitate misfit is discussed in Ref. 19, p. 321.

5) COHERENCY LIMIT

The coherency limit is exceeded in two stages: first, along the edge of the precipitate, and then on the flat faces. The loss of coherency along the thin edge of the precipitate leads to the appearance of a dislocation loop

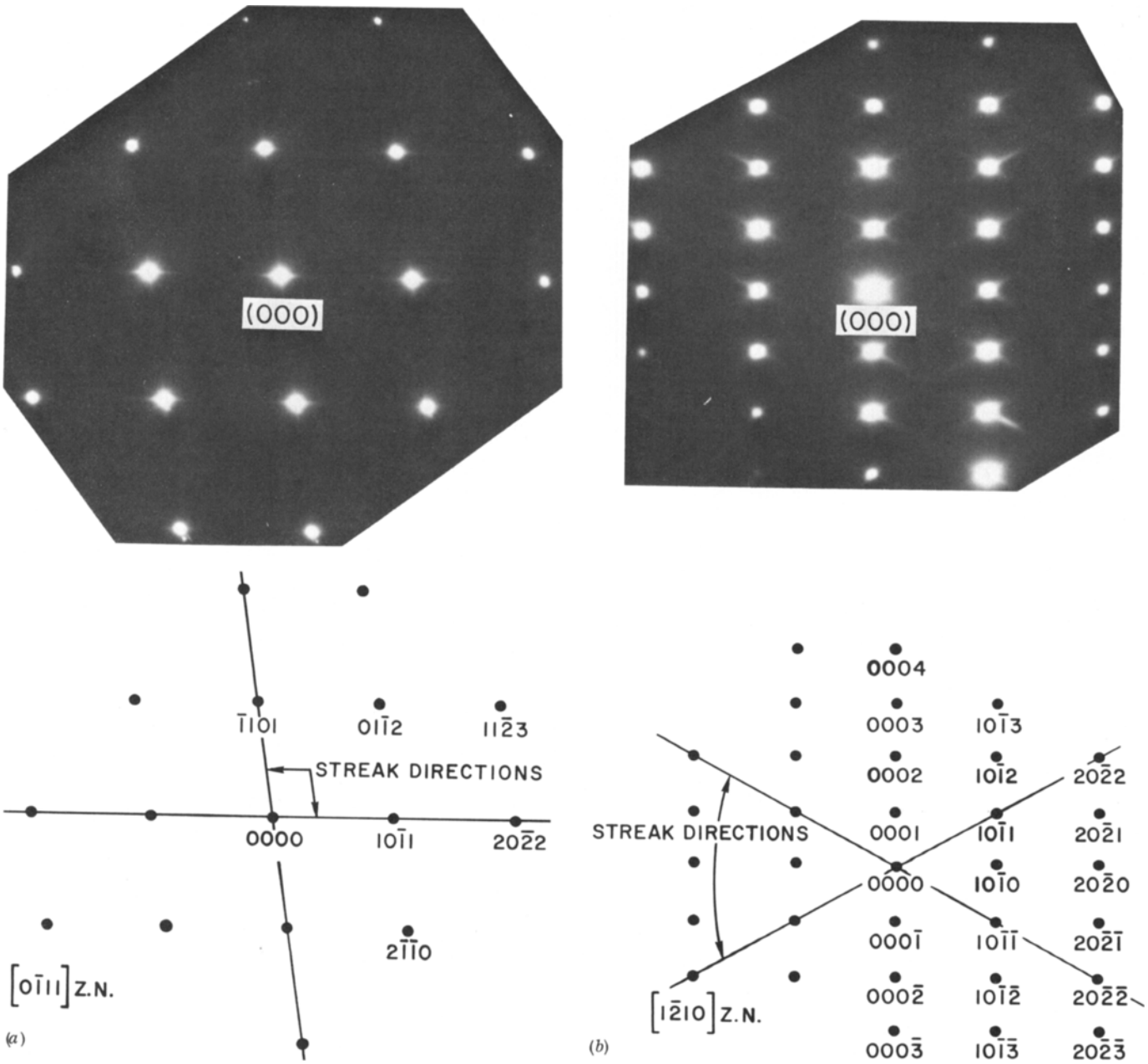

Fig. 4—(*a*) and (*b*) Selected area electron diffraction patterns taken from regions of specimens containing the coherent disk-shaped precipitates. Note the streak directions are always parallel to $\{10\bar{1}1\}$ diffraction vectors.

around the perimeter of the precipitate, as shown in Fig. 9. Diffraction contrast experiments have been conducted to establish the Burgers vector of this dislocation loop; the results of these experiments are shown in Figs. 10(*a*) through (*c*). Fig. 10(*a*) shows that the dislocation is in contrast with a (0002) reflection operating which indicates that it is not a standard $\frac{1}{3}\langle 11\bar{2}0\rangle$ dislocation; further, this result indicates that the Burgers vector of the loop must have a component lying out of the basal plane. The two most common types of dislocations in hexagonal metals which have Burgers vectors with nonbasal components are $\frac{1}{3}\langle 11\bar{2}3\rangle$ and [0001] and these dislocations are denoted **c** + **a** and **c**, respectively. Figs. 10(*b*) and (*c*) show that the dislocation located along the precipitate edge is out of contrast with a $(10\bar{1}0)$ reflection and in contrast with a $(11\bar{2}0)$ reflection. These results indicate that the dislocation must have a Burgers vector of the type **c** + **a** since a **c** type dislocation would be out of contrast with both $(10\bar{1}0)$ and $(11\bar{2}0)$ reflections. Once the dislocation loop has been formed, the growth of the precipitate in a radial direction is arrested and thickening begins, leading to the loss of coherency on the flat faces of the precipitate. Such thickening occurs by the formation and motion of ledges which move across the flat faces of the precipitate, as shown in Fig. 11(*a*). Once the ledge formation and motion process has begun the precipitate is identifiable as Ti_2Cu by selected area electron diffraction. On continued aging the ledge density increases, as shown in Fig. 11(*b*).

6) OVERAGING

During continued aging, the number of ledges per unit area of the precipitate:matrix boundary increases

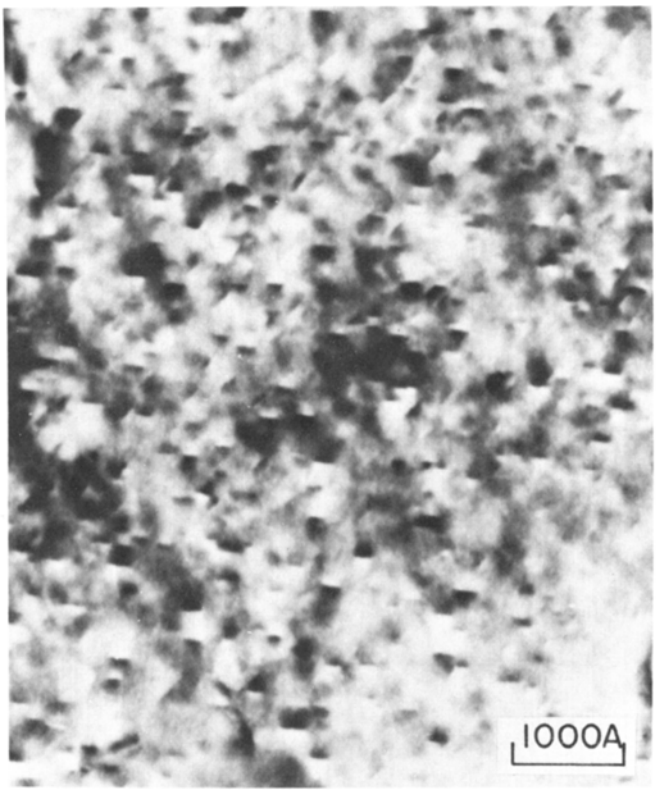

Fig. 5—Very small, coherent precipitates, just after the disk morphology is discernable. Ti-4 pct Cu β-quenched and aged 8 hr at 400°C.

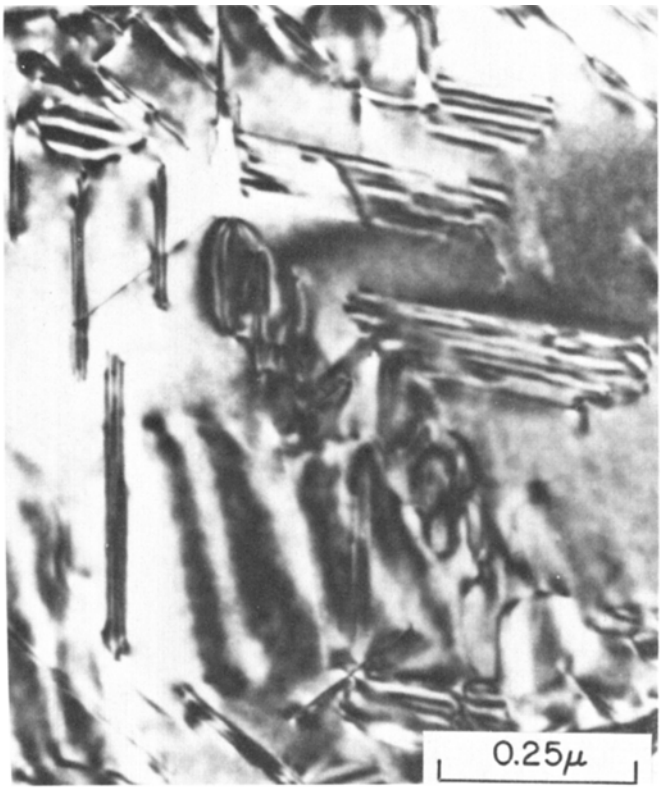

Fig. 6—Extremely large coherent precipitates ~3500Å in diam. Note displacement fringes associated with precipitates that lie thru the foil at an oblique angle.

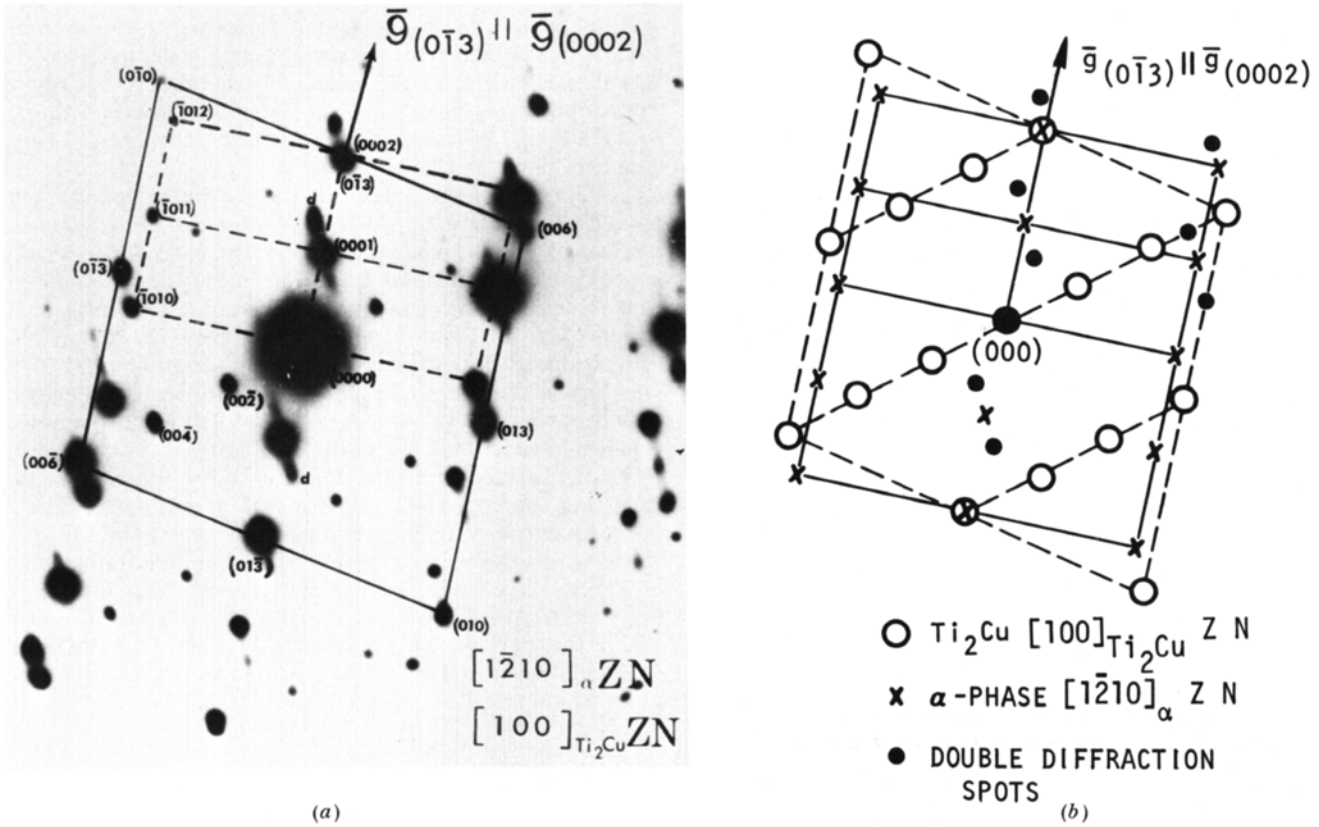

(a) (b)

Fig. 7—(*a*) Selected area electron diffraction pattern in which the $[100]_{Ti_2Cu}$ zone axis is parallel to the $[1\bar{2}10]_{\alpha}$ zone axis and the $(013)_{Ti_2Cu}$ and $(0002)_{\alpha}$ diffraction vectors are coincident. Spots marked '*d*' are double diffraction spots. (*b*) Schematic of 7(*a*) showing the outline of the Ti_2Cu and α-phase zones; symbols are used to identify the reflections as Ti_2Cu, α-phase or double diffraction.

and the boundary begins to approximate a disordered boundary. After still longer aging times the precipitates assume irregular shapes and nonuniform sizes.

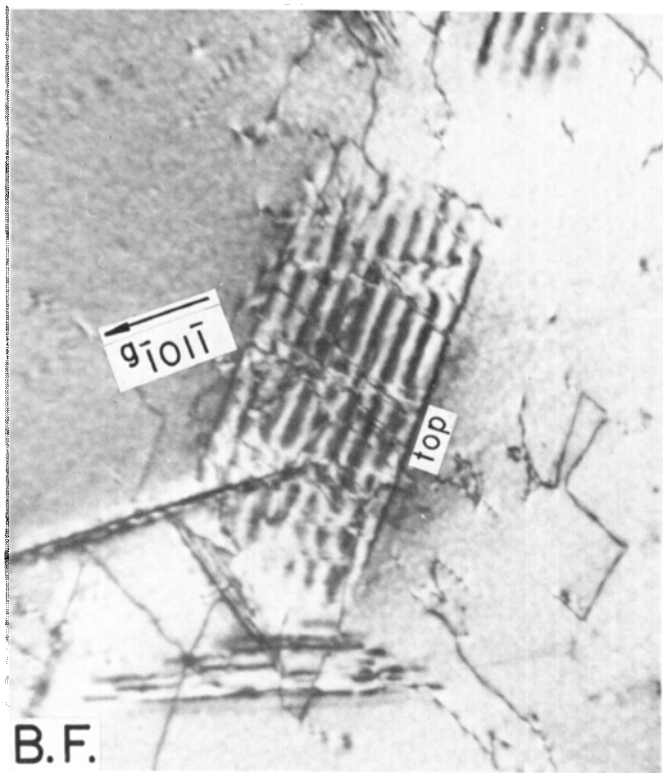

(a)

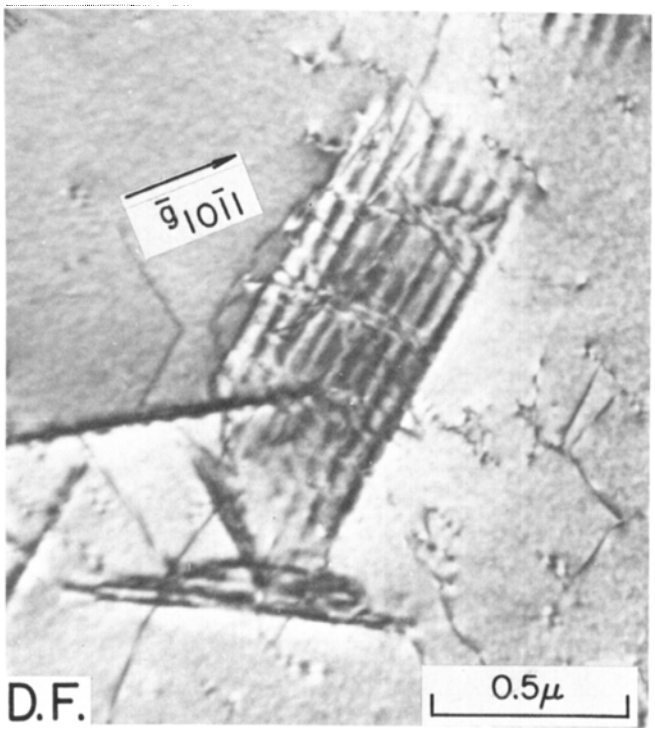

(b)

Fig. 8—Displacement fringe contrast associated with the thin coherent precipitates: (*a*) Bright field, +**g**, showing symmetric fringe system. (*b*) Dark field, −**g**, showing assymmetric fringe system. (*c*) Schematic showing that behavior of fringes in 8(*a*) and (*b*) is consistent with a positive misfit vector.

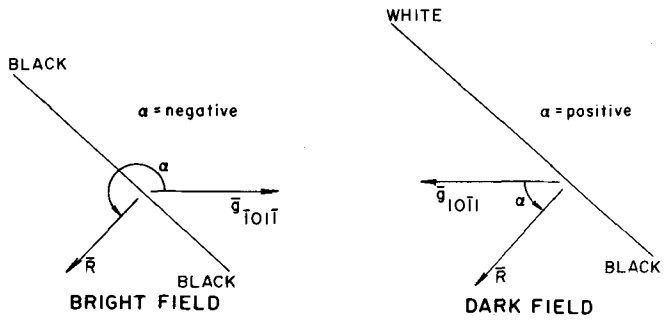

(c)

Fig. 8—Continued

Some of the interphase boundaries exhibit interfacial dislocation arrays, examples of which are shown in Figs. 12(*a*) and (*b*). The precipitates undergo very slow coarsening at temperatures up to 550°C, the highest temperature used in this study. No general recrystallization of the α matrix such as the annihilation of prior martensite plate boundaries by climb or thermally activated glide is observed in any of the alloys after any aging treatment, although limited polygonization was observed in the 6 and 8 pct Cu alloys.

DISCUSSION OF RESULTS

A) Heterogeneously Nucleated Precipitates

The heterogeneous nucleation of precipitates at dislocations has been analyzed by Cahn,[11] Nicholson[12] and by Hornbogen.[13] They have shown that dislocations can catalyze the nucleation of precipitates by relieving a portion of the strain energy associated with the formation of the precipitate, thereby reducing the activation energy barrier for nucleation. The maximum energy reduction is realized when the Burgers vector of the dislocation is parallel to the misfit vector of the precipitate.

In the present study the martensite place boundaries have been identified as the most effective heterogeneous nucleation sites for the semicoherent precipitates. In a previous paper[4] it has been shown that these boundaries consist of arrays of dislocations nearly all of which have Burgers vectors of the type $\frac{1}{3}\langle 11\bar{2}3\rangle$. Examination of the relative disposition of the normal to $\{10\bar{1}1\}$ planes (the direction of misfit of the disk-shaped precipitates) and the Burgers vectors of the **c** + **a** and **a** type dislocations shows that there are always four variants of the precipitate habit plane which make equally large angles with a given **a** Burgers vector, whereas there is only one variant which makes a maximum angle with a given **c** + **a** Burgers vector. Examination of Figs. 1 and 2 indicate that at least two variants of precipitate are always nucleated at the **a** dislocations within the martensite plates, whereas only one variant is nucleated at the **c** + **a** dislocations in the martensite plate boundaries.

B) Uniformly Nucleated Precipitates

The formation of a uniform distribution of coherent, disk-shaped precipitates with densities as high as 10^{17} per cu cm during the aging of supersaturated Ti-Cu solid solutions is similar in many respects to the decomposition of Al-Cu alloys.[13,14] The experimental

results show that the decomposition can be separated into three stages with each stage representing a different state of coherency of the precipitate.

Evidence obtained by following the precipitation reaction from the coherent to the incoherent stage indicates that the fully coherent precipitates are solute-rich regions having the same structure as the matrix. Two additional factors indicate that the coherent precipitate is not Ti_2Cu when the lattice matching across the $\{10\bar{1}1\}$ habit plane is considered, assuming the orientation relation derived from Fig. 7 and other selected area diffraction patterns.

i) A coherent interface requires continuity of the lattice planes across the precipitate/matrix interface, thus if the precipitates were Ti_2Cu, the $(001)_{Ti_2Cu}$ plane would be the interface plane. Comparison of the interplanar angles shows that such a situation results in ~12 deg misorientation between the $\{10\bar{1}1\}_{matrix}$ and $(001)_{Ti_2Cu}$ planes, so that the Ti_2Cu structure could not exist.

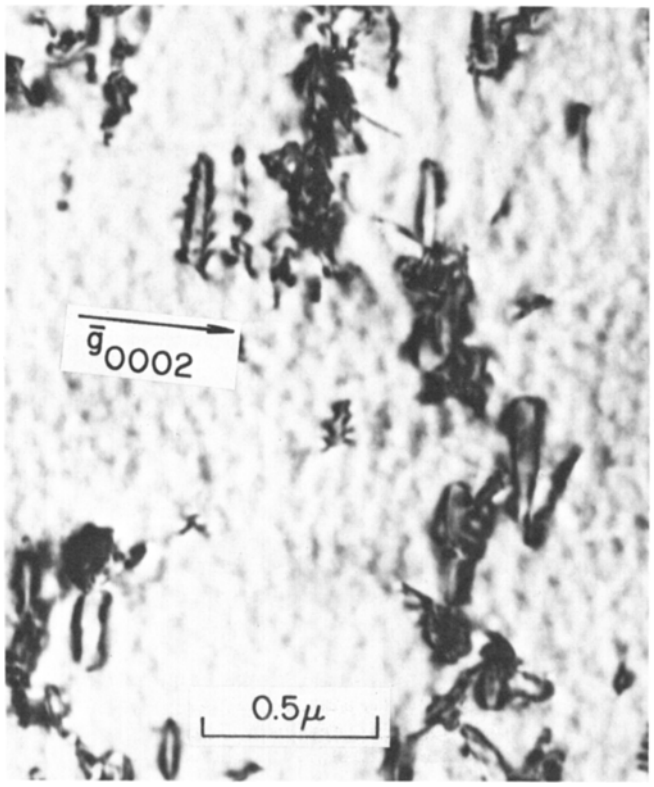

Fig. 9—Heterogeneously nucleated precipitates and semi-coherent uniformly nucleated precipitates which show a line of no contrast normal to $g_{10\bar{1}1}$.

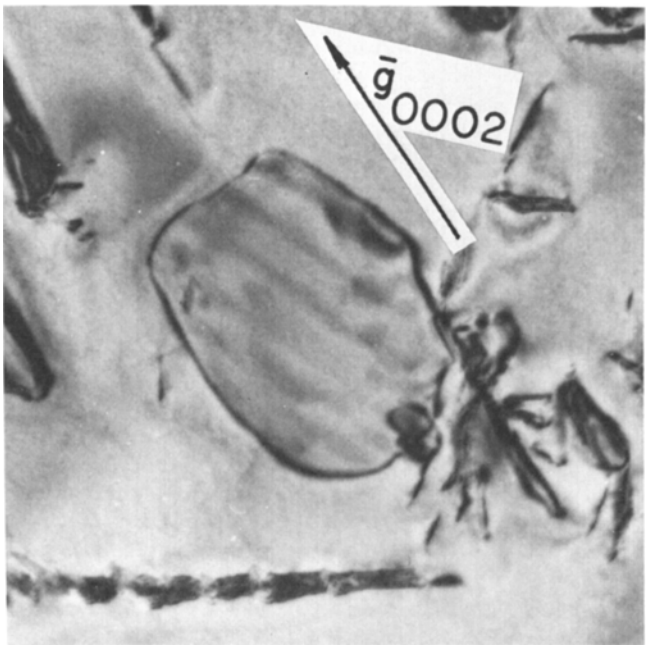

(a)

Fig. 10—A semi-coherent precipitate taken under 3 different contrast conditions. (*a*) g_{0002} showing dislocation loop in contrast. (*b*) $g_{10\bar{1}0}$ showing dislocation loop out of contrast. (*c*) $g_{11\bar{2}0}$ showing dislocation loop in contrast again.

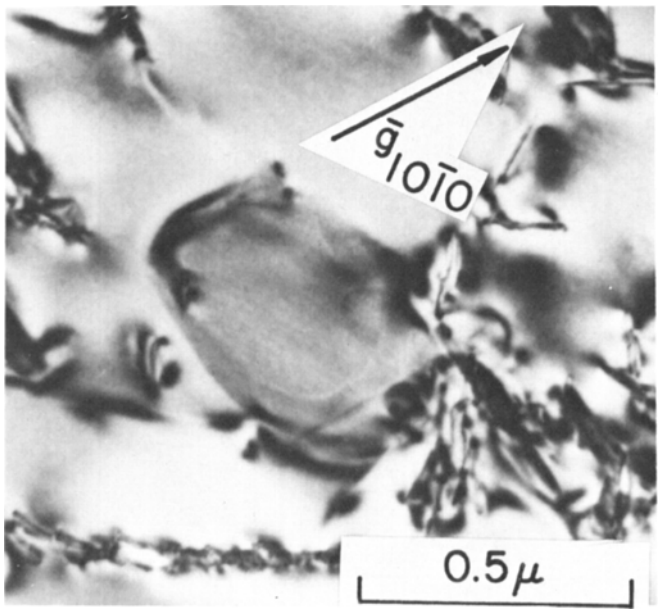

(b)

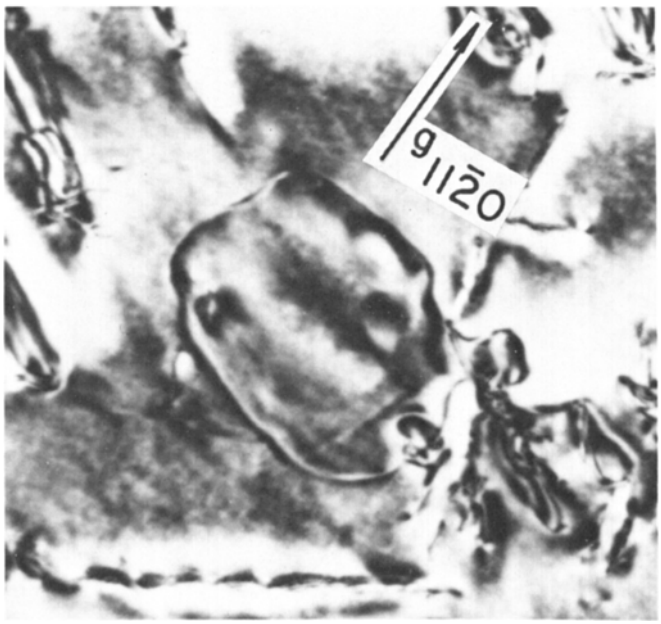

(c)

Fig. 10—Continued

ii) Although the misfit between two anisotropic structures varies with the specific crystallographic direction, the atomic positions in the Ti_2Cu lattice and those in the matrix exhibit a mismatch of >6 pct along any crystallographic direction in the $\{10\bar{1}1\}_{\alpha'}$ habit plane of the plate-shaped coherent precipitates. Such a large mismatch would result in the formation of misfit dislocations in the broad interface with the dislocation spacing being on the order of 50 to 60Å, based on a Brooks[15] type coherency criterion. Fully coherent precipitates with diameters larger than 3500Å have been shown in Fig. 6 so that this observation also indicates that the coherent precipitates are not Ti_2Cu. No information regarding the exact nature of the atomic arrangements within the precipitates has been obtained in the present study and thus the possibility of ordering within the solute-rich zones cannot be ignored.

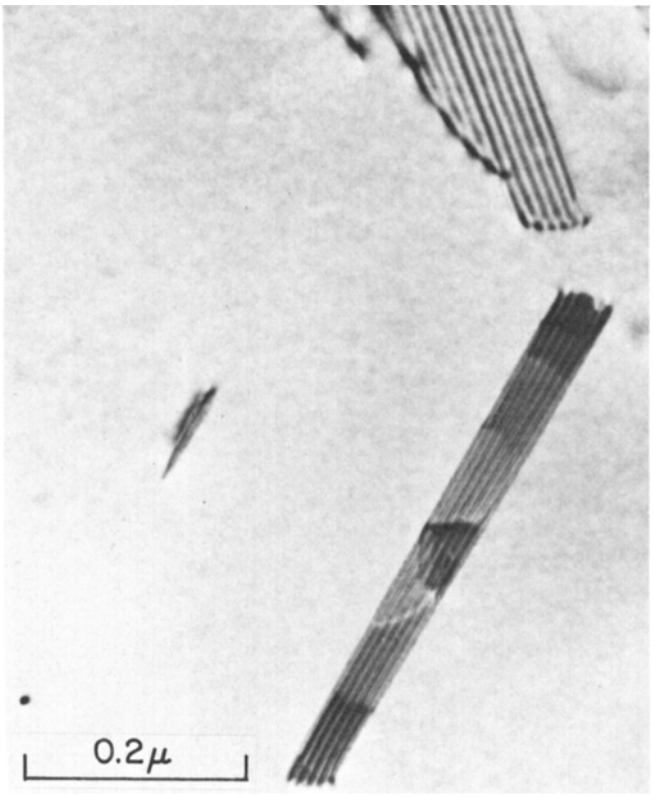

(a)

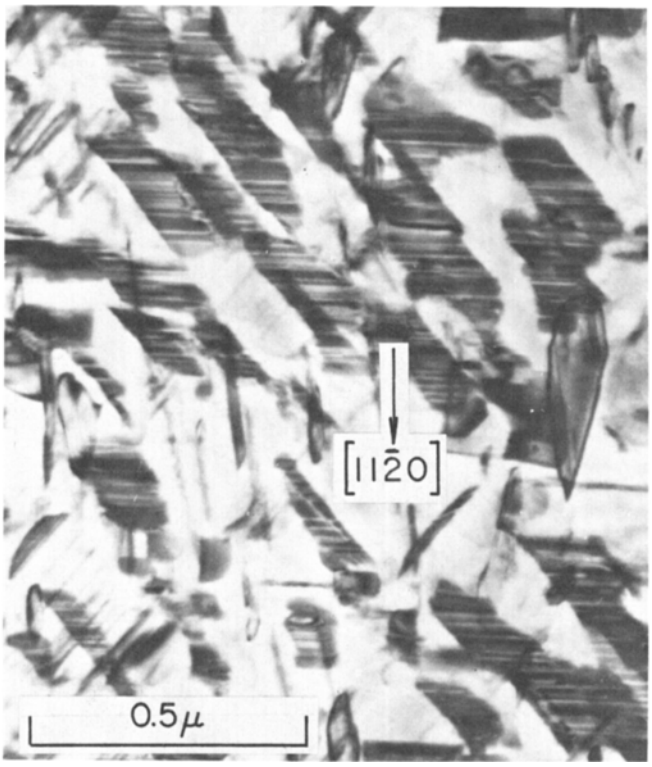

(b)

Fig. 11—(*a*) Semi-coherent precipitate containing several ledges. (*b*) Very high density of ledges which have become straight and lie normal to $\langle 11\bar{2}0\rangle_{\alpha}$.

The thin fully coherent precipitates show evidence of coherency strain contrast, as shown in Fig. 5, starting with the early stages of formation until the coherency limit is exceeded. Nabarro[16,17] has analyzed the strain energy associated with precipitates of varying shapes and has shown that for ellipsoids of revolution having semiminor axes R, and a semimajor axis y that the strain energy is minimized when $R \gg y$, *i.e.*, when the precipitate approximates to a thin disk. Thus, the observed coherency strain contrast and the disk-like morphology indicate that the precipitate/matrix misfit is sizable. The exact misfit cannot be calculated, however, since the precipitates are solute rich zones and no lattice parameter data is available for a calculation of the misfit $\Delta a/a$.

The $\{10\bar{1}1\}$ habit plane of the disks cannot be accounted for on the basis of anisotropic elasticity since in the case of α-titanium [unlike the (100) θ' habit in Al-Cu] the strain energy is not minimized for such a habit plane, as shown recently by calculations done by Alers.* As an alternative, it is suggested that the surface energy is minimized by this precipitate habit plane, thereby minimizing the sum of the misfit and surface free energies associated with the precipitate. A low interfacial energy is also consistent with the formation of solute-rich zones prior to the formation of the equilibrium Ti_2Cu phase, since this factor reduces the height of the energy barrier for nucleation of the coherent precipitate relative to the energy requirements for the nucleation of Ti_2Cu.

*Alers[18] has recently calculated the angular dependence of the modulus associated with the displacement of a sheet of material normal to itself. His calculations show that this modulus is *not* a minimum in the direction normal to $\{10\bar{1}1\}$.

The displacement fringes that appear after continued aging are shown in Figs. 8(*a*) and (*b*) at the precipitate: matrix interface and, as has been stated earlier, the appearance of these fringes is not preceded by a perceptible thickening of the precipitate. Such fringes indicate that the precipitate misfit in a direction normal to the $\{10\bar{1}1\}$ habit plane has increased during further aging. This is best seen by recalling that since the phase shift, α, introduced by the precipitate is defined by the expression $\alpha = 2\pi\mathbf{g}\cdot\mathbf{R}$, an increase in the precipitate misfit vector R causes an increase in α, rendering it large enough to produce the observed displacement fringe contrast.[19] The value of R is proportional to the thickness, t, of the precipitate and to the specific misfit, ϵ. Thus, the occurrence of displacement fringes without thickening of the precipitate can be interpreted as evidence for an increase in ϵ and such an increase is good evidence that the precipitate

composition changes as aging proceeds. The formation of the **c** + **a** dislocation loop around the precipitate perimeter as shown in Figs. 9 and 10(*a*) through (*c*) is also a direct consequence of the increase in precipitate misfit. Using the Brooks criterion, the critical mismatch in the thickness direction between the precipitate and the matrix corresponding to the formation of this **c** + **a** misfit dislocation is 8 to 10 pct. This increase in misfit with no attendant thickening of the zone can be interpreted in terms of copper enrichment, producing a substantial increase in the lattice parameter of the precipitate.

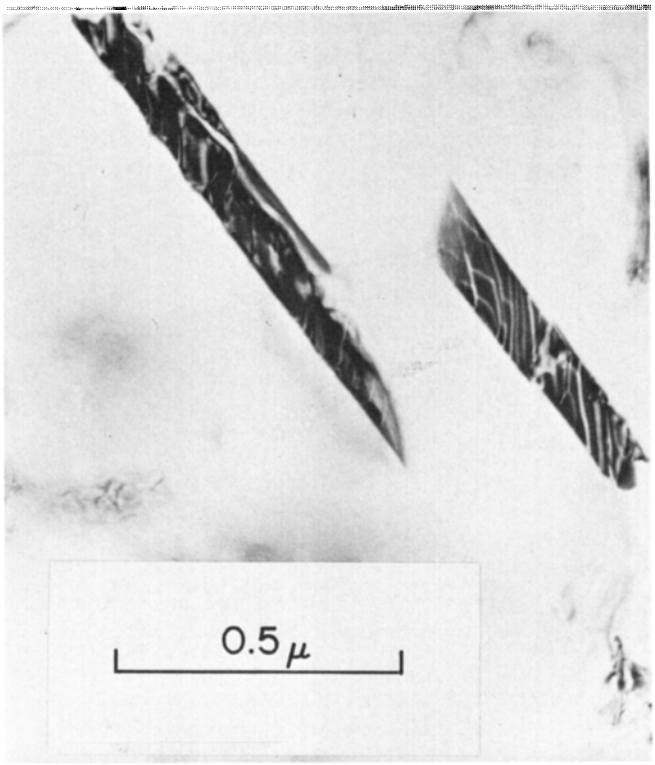

(*a*)

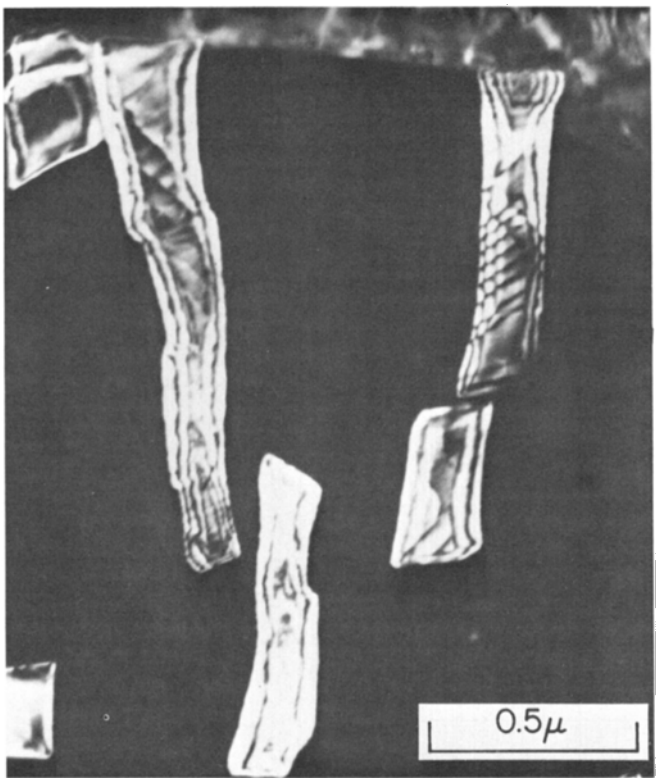

(*b*)

Fig. 12—(*a*) and (*b*) Two examples of the interphase boundary dislocations which are observed on many of the incoherent Ti_2Cu particles after long aging times (> 72 hr) at 550°C. (*b*) is a dark field micrograph using a Ti_2Cu reflection.

The growth of the coherent precipitate in the radial direction only, lends support to the earlier suggestion that the $\{10\bar{1}1\}$ habit plane results from a minimization of surface energy, since thickening by any mechanism other than synchronous climb introduces steps which are not $\{10\bar{1}1\}$ segments. Further, it has been shown that there is sizable precipitate misfit in the thickness direction and the total strain energy associated with each precipitate can be minimized by making R much greater than y. Minimization of the elastic strain energy imposes an additional constraint on the thickening of the coherent precipitate.

Once the **c** + **a** dislocation loop is formed around the perimeter of the precipitate, the thickening of the precipitate proceeds by the formation and the motion of ledges across the flat precipitate interfaces such as those shown in Figs. 11(*a*) and (*b*). At the same time the radial growth of the precipitates is arrested because this process requires the climb of the **c** + **a** dislocation which is a slow process. The loss of coherency along the edges of the precipitate releases the elastic constraint on the precipitate and allows it to assume a '**c**/**a**' ratio approximating that of Ti_2Cu. The detection of Ti_2Cu reflections always quickly succeeds the loss of coherency of the precipitate. If an intermediate precipitate were involved in the transition from the coherent precipitates to the formation of Ti_2Cu, it must be very transient in nature. The ~12 deg angular mismatch between the $\{10\bar{1}1\}$ matrix and the (001) precipitate interfacial planes can be accommodated by the formation of a series of ledges in a manner similar to that discussed by Aaronson and Laird[20] for the θ' phase in Al-Cu alloys. The kinetics of the motion of these ledges will be aided by rapid diffusion along the ledge since it represents the limiting case of a disordered boundary. The passage of these disordered boundaries allows rapid readjustment of atom positions, and the precipitate then assumes the equilibrium Ti_2Cu structure. The observed shift from radial growth to the thickening of the precipitates results from a combination of the following factors:

i) The requirement for climb of the **c** + **a** dislocation loops which limits the radial growth.

ii) The angular mismatch between the precipitate and matrix interfacial planes which makes ledge formation favorable.

iii) The enhanced rate of diffusion along the ledges.

As the number of ledges increases, they become straight and are aligned along directions that are perpendicular to the $\langle 11\bar{2}0\rangle_{\alpha'}$ close-packed directions, as shown in Fig. 11(*b*). The extreme straightness and the parallel nature of these ledges suggests that their shape and orientation are influenced by the crystallography of the precipitate or that of the matrix, or both.

As thickening proceeds, the density of the ledges is observed to decrease and the formerly flat interfaces become curves. Since unit ledges lose their identity in

a disordered boundary, the decrease in ledge density reflects the increased disorder of the precipitate: matrix interface. The remaining ledges must be "superledges" or ledges several lattice spacings in height. At this stage of the aging sequence the precipitate has been identified as Ti_2Cu by selected area electron diffraction, Fig. 7, and a disordered boundary would be expected in view of the poor lattice matching between Ti_2Cu and the α' phase. The precipitates which have interfacial dislocations associated with them such as those shown in Fig. 12(*a*) and (*b*) generally have planar facets which contain the dislocations. The plane of the facets apparently represents a plane of low surface energy, the lattice misfit being accommodated by the dislocations in the interphase boundary.

C) Summary of the Stages of Formation of the Uniformly Nucleated Precipitate

The development of the uniformly nucleated precipitate can thus be characterized by the following three stages.

i) The formation of the solute-rich coherent regions which on slightly prolonged aging develop into thin, coherent, plate-shaped precipitates having a hexagonal structure of larger lattice parameter than the matrix, resulting in a positive misfit.

ii) The partial loss of coherency of the fully coherent precipitate by the formation of a **c** + **a** dislocation loop around the perimeter of the precipitate.

iii) The complete loss of coherency of the stage ii) precipitate which can at this point be identified as Ti_2Cu by selected area diffraction as shown in Fig. 7.

These stages of precipitation in Ti:Cu alloys are distinct from those observed in Al alloys because the changes in the nature of the precipitate in Ti:Cu occur *in situ*, *i.e.* by a monotropic transformation, whereas in Al alloys each successive precipitate in the sequence is separately nucleated and growth occurs while the preceding precipitate goes back into solution.[13,14]

CONCLUSIONS

1) During aging, supersaturated solid solutions of Ti:Cu decompose by two distinct processes: the heterogeneous nucleation and growth of precipitates at interfaces and dislocations, and the uniform nucleation of thin coherent precipitates.

2) The particular variants of the precipitates nucleated heterogeneously at dislocations are those for which the Burgers vector of the dislocation can accommodate the largest portion of the precipitate misfit.

3) The uniformly nucleated disk-shaped precipitates are initially coherent and lose coherency during aging in two stages: by the formation of a **c** + **a** dislocation loop around the perimeter of the disk and then by the formation and motion of ledges across the broad faces of the disk, resulting in incoherent Ti_2Cu in the final "overaged" state.

ACKNOWLEDGMENTS

The authors gratefully acknowledge the helpful discussions of B. S. Hickman, G. A. Alers and H. I. Aaronson. We also wish to thank E. H. Wright for assistance in preparing the figures for the manuscript. This work was funded under AEC Contract [AT(45-1)-2225-T13 (RLO-2225-T13-4)].

REFERENCES

1. D. N. Williams, R. A. Wood, H. R. Ogden, and R. I. Jaffee: *Trans. TMS-AIME,* 1960, vol. 218, p. 787.
2. W. C. Gallaugher, R. Taggart, and D. H. Polonis: *Trans. TMS-AIME,* 1965, vol. 233, p. 944.
3. M. J. Blackburn and J. C. Williams: *Trans. TMS-AIME,* 1967, vol. 239, p. 287.
4. J. C. Williams, R. Taggart, and D. H. Polonis: *The Science, Technology and Application of Titanium,* R. Jaffee and N. Promisel, eds., pp. 733-43, Pergamon Press, 1970.
5. G. D. Preston: *Phil. Mag.,* 1938, vol. 26, p. 855.
6. A. Guinier: *Ann. Phys.,* 1939, vol. 12, p. 161.
7. J. Silcock: *Acta Met.,* 1958, vol. 6, p. 481.
8. M. J. Blackburn and J. C. Williams: *Trans. TMS-AIME,* 1968, vol. 242, p. 2461.
9. M. F. Ashby and L. M. Brown: *Phil. Mag.,* 1963, vol. 8, p. 1083.
10. M. F. Ashby and L. M. Brown: *Phil. Mag.,* 1963, vol. 8, p. 1649.
11. J. W. Cahn: *Acta Met.,* 1957, vol. 5, p. 168.
12. R. B. Nicholson: *Electron Microscopy and Strength of Crystals,* G. Thomas and J. Washburn, eds., p. 861, Interscience, New York, 1963.
13. E. Hornbogen: *Aluminium,* 1967, vol. 43, p. 19.
14. A. Kelly and R. B. Nicholson: *Prog. Mater. Sci.,* 1963, vol. 10, p. 151.
15. H. Brooks: *Metal Interfaces,* p. 20, ASM, Cleveland, Ohio, 1952.
16. F. R. N. Nabarro: *Proc. Phys. Soc.,* 1940, vol. 52, p. 90.
17. F. R. N. Nabarro: *Proc. Roy. Soc.,* 1940, vol. A175, p. 519.
18. G. A. Alers: North American Rockwell Science Center, Thousand Oaks, Calif., private communicaiton, 1970.
19. P. B. Hirsch, A. Howie, R. B. Nicholosn, D. W. Pashley, and M. J. Whelan: *Electron Microscopy of Thin Crystals,* p. 34, Butterworths, London, 1965.
20. H. I. Aaronson and C. Laird: *Trans. TMS-AIME,* 1968, vol. 242, p. 1393.